Eur. Phys. J. B **58**, 107–113 (2007)
DOI: 10.1140/epjb/e2007-00207-3

THE EUROPEAN PHYSICAL JOURNAL B

Coherence transition in granular $YBa_2Cu_3O_{7-\delta}$, $YBa_2Cu_{2.95}Zn_{0.05}O_{7-\delta}$, and $YBa_{1.75}Sr_{0.25}Cu_3O_{7-\delta}$ superconductors

R. Menegotto Costa[1], L. Mendonça Ferreira[2], V.N. Vieira[3], P. Pureur[2,a], and J. Schaf[2]

[1] Instituto de Ciências Exatas e Tecnológicas, Centro Universitário Feevale, 93510-250 Novo Hamburgo, RS, Brazil
[2] Instituto de Física, Universidade Federal do Rio Grande do Sul, 91501-970 Porto Alegre, RS, Brazil
[3] Instituto de Física e Matemática, Universidade Federal de Pelotas, 96010-900 Pelotas, RS, Brazil

Received 20 March 2007 / Received in final form 25 June 2007
Published online 1st August 2007 –

Abstract. We have studied experimentally the electrical magneto-conductivity near the superconducting transition of $YBa_2Cu_3O_{7-\delta}$, YBa_2 $(Cu_{2.95}Zn_{0.05})O_{7-\delta}$ and $Y(Ba_{1.75}Sr_{0.25})Cu_3O_{7-\delta}$ polycrystalline samples. The measurements were performed in magnetic fields ranging from 0 to 400 Oe applied parallel to the current orientation. The results show that the resistive transition of these systems proceeds in two stages. The pairing transition occurs at the bulk critical temperature T_c, where superconductivity is stabilized within small and homogeneous regions of the sample generically called grains. The regime of approach to the zero resistance state reveals the occurrence of a coherence transition at a lower temperature T_{c0}. This transition is related to the connective nature of the granular samples and is controlled by fluctuations of the order-parameter phase of individual grains. Our experiments show that the Zn-doping, besides depressing the pairing critical temperature, strongly enlarges the temperature range dominated by effects related to the coherence transition. The substitution of Ba by Sr causes only a small reduction of T_c, but also enhances significantly the effects related to the grain coupling phenomenology. In general, our results indicate that these impurity substitutions in $YBa_2Cu_3O_{7-\delta}$ produce or magnify the granularity at a microscopic level, enhancing the effects of phase fluctuations in the conductivity near the transition.

PACS. 74.40.+k Fluctuations – 74.72.Bk Y-based cuprates – 74.81.Bd Granular, melt-textured, amorphous, and composite superconductors

1 Introduction

The sintered samples of the high temperature superconducting cuprates (HTSC) show a pronounced granular character that plays an important role in many of their properties. It is well-known from detailed investigations of thin-film bicrystals that the boundaries between crystallites behave as Josephson junctions that are extremely sensible to applied magnetic fields [1,2]. These metallurgical grain boundaries are responsible for the disappointing low critical currents observed in standard polycrystalline HTSC samples [3]. In addition, phase separation [4,5] and a variety of defects inside crystals, ranging from impurities to micro-cracks, may also locally depress the superconducting order parameter [6], thus enhancing the overall granular character of superconductivity in polycrystalline HTSC.

The resistive transition of sintered samples of the HTSC shows a characteristic two stage behavior [7–9]. When the temperature is decreased, one first observes the pairing transition, where superconductivity is stabilized in some small and homogeneous regions of the sample. These superconducting grains may not necessarily be coincident with the crystallographic grains [6,10]. The pairing transition occurs at a temperature practically identical to the bulk T_c. In lower temperatures, the resistivity is described by a percolation-like process related to the activation of weak links between the superconducting grains [8–11]. The resistivity becomes zero at the coherence transition [9–11] that occurs in a critical temperature T_{c0} well below T_c. This transition is dominated by the fluctuating phases of the Ginzburg-Landau (G-L) order parameter of individual grains that couple into a long range ordered state, leading to the zero resistance state [9–11].

The simplest description of this process when it occurs in the presence of a magnetic field is given by a generalized version of the pair tunneling Hamiltonian [12]

$$H = -\sum_{i,j} J_{ij} \cos\left(\theta_i - \theta_j - A_{ij}\right), \qquad (1)$$

where the sums run over nearest neighbor grains, J_{ij} is the coupling energy between grains i and j, and θ_i is the phase of the G-L order parameter in grain i. The gauge

[a] e-mail: ppureur@if.ufrgs.br

factor A_{ij} is given by

$$A_{ij} = \frac{2\pi}{\Phi_0} \int_i^j \boldsymbol{A} \cdot d\boldsymbol{l}, \tag{2}$$

where Φ_0 is the flux quantum and the line integral for the vector potential is evaluated between the centers of grains i and j. The model represented by equation (1) belongs to the 3D-XY class with nontrivial (associated to frustration) disorder [8]. Frustration is consequence of a random distribution of the factors A_{ij} [12,13]. In this case, one has the gauge glass version of the model represented by equation (1). Frustration may also be introduced as in the chiral glass model [14] when positive and negative values for the couplings J_{ij} are present on a nearly equal footing. Negative J_{ij} are characteristic of π-junctions in d-wave superconductors [15]. These anomalous couplings also occur when magnetic impurities exist in the dielectric layer forming the junction [16,17].

The coherence transition has been studied experimentally by means of careful resistivity versus temperature measurements in many granular samples of the HTSC [9, 11,18–23]. In several of these experiments, magnetic fields were applied parallel or perpendicular to the current orientation. Specific heat results were also used to study this transition in polycrystalline $YBa_2Cu_3O_{7-\delta}$ (Y123) and Zn-doped Y123 samples [24]. These studies show that in the regime of approach to the zero resistance state the conductivity diverges as a power law of the reduced temperature $(T - T_{c0})/T_{c0}$. The values found for the conductivity critical exponents λ are much larger than those expected with basis on the homogeneous 3D-XY model [9]. This result indicates that disorder is relevant for the criticality in this problem. In the ordered case one would expect $\lambda \approx 1/3$ [25]. This exponent is observed in the fluctuation regime above the pairing transition in sintered [26] and single crystal [27,28] samples of the HTSC. In granular samples, $\lambda \approx 3$ and $\lambda \approx 4$ have been usually found near the coherence transition [9,18–21]. In addition to $\lambda \approx 3$, some authors also report the observation of the exponent $\lambda \approx 1.3$ [22,23].

In this article we report a study of the resistive transition in polycrystalline Y123, pure and containing Zn or Sr impurities. Emphasis is given on the role of impurities. It is known that both of these dopants cause sizeable modifications in the electronic properties of Y123. The Zn is substitutional to the Cu atoms in the superconducting Cu-O_2 planes and causes a strong reduction of T_c [29]. Magnetic moments are stabilized around the Zn impurities [30], and some local magnetic ordering may be produced [30,31]. The Sr impurities are substitutional to the Ba atoms [32,33]. In this case a gradual reduction of T_c, which depends linearly on the impurity concentration, is verified. For both impurities, however, a strong enhancement of the granularity effects in transport and magnetic properties is observed [34]. One may suppose that doping effectively induces granularity at the microscopic level and weakens the coupling between larger grains. One consequence of this fact is the enhancement of phase fluctuations effects in the resistive transition of doped samples [35] that could be regarded as model systems for studying the coherence transition. Particularly, in the case of the Zn-doped sample, the proposed suppression of the superconducting carrier density around the Zn impurities, known as the "Swiss-cheese model" [36], is expected to be rather efficient to enhance the granularity effects at the microscopic level.

Our results allow the determination of the critical exponents and amplitudes for the fluctuation conductivity near the coherence transition of the investigated samples. Critical exponents are sample independent confirming prior studies [9,20,21]. The amplitudes, however, are extremely sensible to the degree of granular disorder. Moreover, the critical amplitudes increase continuously with the magnetic field intensity. A universal scaling was obtained for the fluctuation conductivity in the temperature range that precedes the coherence transition. The associated reduced temperature depends both on T_{c0} and T_c. This scaling is justified in terms of the general vortex-glass theory [37].

2 Experimental details

Using the standard solid state reaction and sintering techniques, we have prepared two polycrystalline samples of $YBa_2Cu_3O_{7-\delta}$, labeled Y123:a and Y123:b, one of $YBa_2(Cu_{2.95}Zn_{0.05})O_{7-\delta}$ (Y123:Zn), and one of $Y(Ba_{1.75}Sr_{0.25})Cu_3O_{7-\delta}$ (Y123:Sr). Powders of Y_2O_3, $BaCO_3$, CuO, $SrCO_3$ and ZnO having 99.99% purity or better were mixed in adequate proportions to prepare the samples. The initial calcination was performed in 950 °C in zirconia crucible under oxygen atmosphere. The resulting pellets were finely powdered, loosely pressed and heated again to 950 °C during several hours in oxygen atmosphere and ground again. After this intermediate process, a final sinterization was done of the powders pressed at 3 ton/cm^2 into disks of thickness about 2 mm and diameter of 9 mm. The sinterization was performed for 24 h in 930 °C. Subsequently, the samples were slowly cooled down to 450 °C and submitted to a final annealing at this temperature for further 24 h under oxygen atmosphere. The resulting samples were characterized by X-ray diffraction that showed they are single-phase and have the expected lattice parameters. Densities about 80% of the ideal values were obtained. Examination with optical microscopy showed a typical ceramic morphology with crystallite sizes in the range 1–10 μm Specimens in the form of parallelepiped, adequate for resistivity measurements, were cut out from the sintered buttons with a diamond saw. Typical sample dimensions are $1 \times 1 \times 9$ mm^3.

The resistivity experiments were performed with a low-frequency AC technique based on an ESI automatic ratio transformer that balances a compensation circuit, and a lock-in amplifier that operates as a null detector. Relative sensitivities around 10^{-5} were obtained in the resistivity measurements. Current densities of 0.1 A/cm^2 and 1 A/cm^2 were employed. Four contacts in the form of stripes perpendicular to the current axis were silver

painted on one of the largest samples' surfaces. The contact resistances ranged between 1 and 3 ohms. Several magnetic field intensities up to 400 Oe could be applied parallel to the current direction. In-field measurements were carried out according to the field cooled (FC) prescription. For a given field magnitude at least two resistivity versus temperature runs were accomplished, one for decreasing temperatures, the other for increasing temperatures. In some cases more than two runs were needed to make a reliable quantitative analysis of the results. Temperature was measured with a Pt sensor allowing a resolution better than 2 mK. Measurements were concentrated in the temperature range encompassing the superconducting transition. A large number of data points were automatically recorded while the temperature drifted at rates never exceeding 5 K/h. The temperature derivative of the resistivity could be numerically determined with a good accuracy.

3 Results

Figure 1 shows $d\rho/dT$ as a function of temperature for the granular Y123:a, Y123:Sr and Y123:Zn samples at zero applied field. The two-stage nature of the superconducting transition in these systems is apparent from these results. The position of the main peak in $d\rho/dT$, which is denoted as T_P, is approximately coincident with the pairing critical temperature T_c [38]. The effects of granularity dominate the resistivity behavior from the bulk T_c down to the onset of the zero resistance state. We observe the strong depression of T_c as consequence of Zn substitution in the Cu sites of the CuO_2 planes. It is also evident that the Zn substitution causes a significant enlargement of the width of the resistive transition, indicating that granularity is enhanced by Zn-doping. We note a small but sizeable reduction of T_c for the Y123:Sr sample. The pairing critical temperatures determined from the position of T_P are 92.3 K, 92 K, 90 K and 79.4 K for Y123:a, Y123:b, Y123:Sr and Y123:Zn, respectively.

Figure 2 shows the resistive transition for the Y123:a and Y123:b samples in several applied fields. Upper panels present resistivity versus temperature plots, whereas in lower panels $d\rho/dT$ results are shown in the same temperature range. Figure 3 shows similar measurements for the Y123:Zn and Y123:Sr samples. The applied magnetic fields practically do not affect the shape of the curves in the temperature range above the main peak in $d\rho/dT$. Below T_P, and down to the zero-resistance state, the resistivity of these granular samples is strongly field-dependent. Since the field is systematically applied parallel to the current, dissipation effects due to the flow of Abrikosov vortices are minimized. Thus, the field induced enlargement of the resistive transition in our samples is an effect directly related to granularity. Indeed, an applied magnetic field is expected to enhance the granular character of the samples by weakening the junctions between grains.

We separate the contribution of thermal fluctuations to the conductivity by using a method based on the Kouvel-

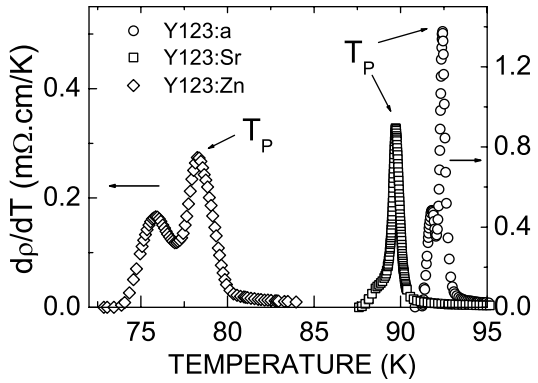

Fig. 1. Temperature derivative of the resistivity near T_c at zero applied field for the Y123:b, Y123:Sr and Y123:Zn samples. The position of the maximum in $d\rho/dT$, denoted as T_P, corresponds approximately to the intragrain pairing transition. The vertical scale at left applies only to the Y123:Zn sample.

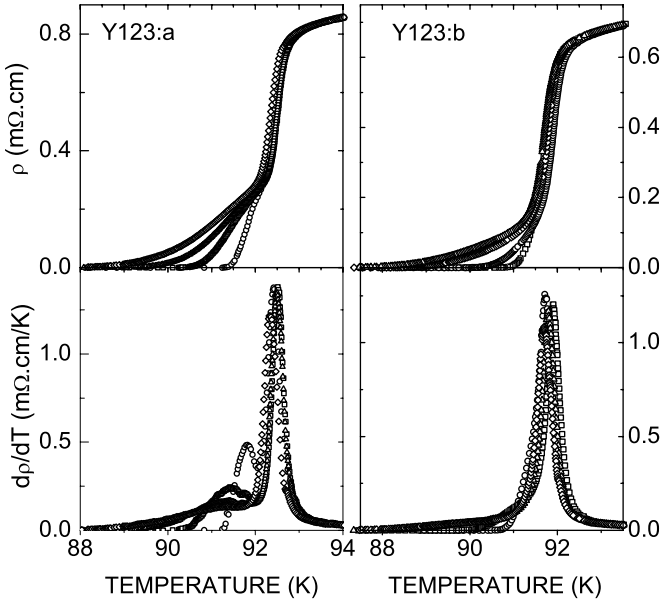

Fig. 2. The resistive transition for the Y123:a and Y123:b samples under magnetic fields applied parallel to the current. Field magnitudes are 0, 10, 50 and 200 Oe for both samples. The transition width enlarges as the field increases. Upper panels represent resistivity versus temperature measurements, whereas the lower panels show the corresponding temperature derivatives.

Fischer analysis of critical phenomena [39]. We numerically determine the quantity [26]

$$\chi_\sigma = -\frac{d}{dT} \ln \Delta\sigma, \tag{3}$$

where $\Delta\sigma$ is the fluctuation conductivity, given by

$$\Delta\sigma = \sigma - \sigma_R. \tag{4}$$

In equation (4), σ is the measured conductivity and the subtracted regular term is estimated by extrapolating the high-temperature behavior, $\sigma_R^{-1} = a + bT$, down to the region of the transition.

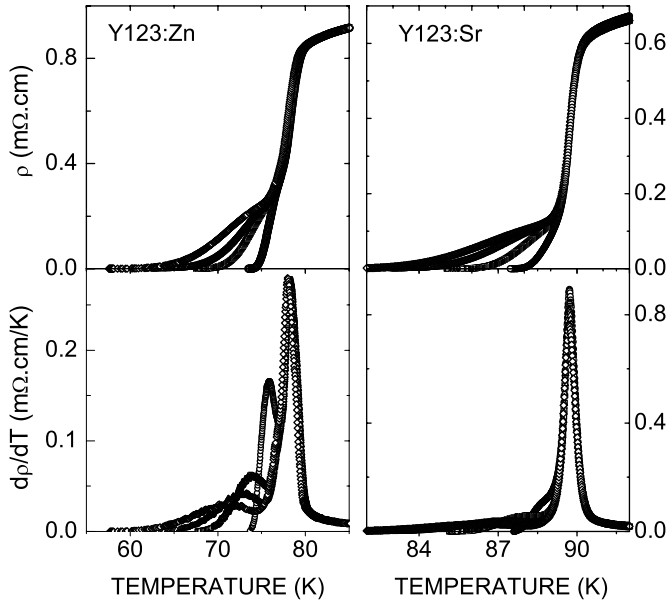

Fig. 3. The same as Figure 2, but for the Y123:Zn and Y123:Sr samples.

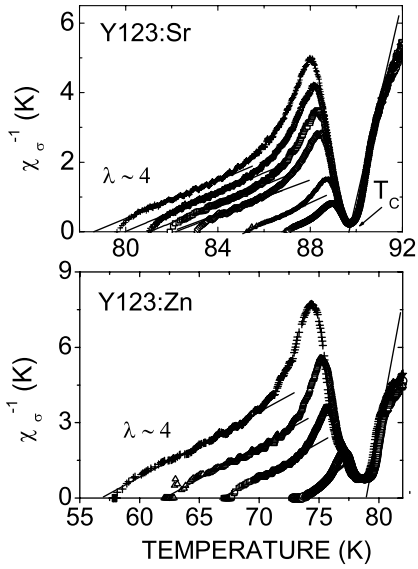

Fig. 4. Resistive transition for the Y123:Sr and Y123:Zn samples represented as χ_σ^{-1} versus temperature (see text) in several applied fields. Fields are 2, 10, 50, 100, 200, 400 Oe for Y123:Sr and 0, 10, 50, 200 Oe for Y123:Zn. The transition enlarges regularly with increasing field. The straight lines correspond to fits to equation (6) with the quoted exponent. Also represented is the position T_P of the main peak in $d\rho/dT$.

Assuming that the coherence transition occurs at a critical temperature T_{c0} near the onset of the zero resistance state, one expects that $\Delta\sigma$ diverges as a power law when the temperature approaches T_{c0} from above, that is,

$$\Delta\sigma = A\,(T - T_{c0})^{-\lambda}\,. \tag{5}$$

From the substitution of equation (5) in equation (3), we obtain that

$$\chi_\sigma^{-1} = \frac{1}{\lambda}\,(T - T_{c0})\,. \tag{6}$$

Thus, the identification of a linear regime in plots of χ_σ^{-1} versus T in the temperature region relevant to the coherence transition (near the zero resistance state) allows the simultaneous determination of the critical temperature T_{c0} and the critical exponent λ.

In Figure 4 we show the resistive transition of Y123:Sr (upper panel) and Y123:Zn (lower panel) represented as χ_σ^{-1} vs. T in some of the studied fields. Similar results were obtained for the Y123:a and Y123:b samples. The two-stage character of the transition is still more evident in the representation of Figure 4. Above the deep minimum where T_c is located, the conductivity is enhanced by superconducting thermal fluctuations in the normal phase. The quantity χ_σ^{-1} is almost field-independent in this region, which precedes the pairing transition. Conductivity fluctuations in this case are governed by the 3D-XY-E universality class [26–28]. The region of validity of this critical regime and the extrapolated T_c are indicated by a thin straight line in Figure 4, for both compounds.

In the present paper, however, we focus on the scaling of the conductivity near the zero resistance state. Below the minimum, χ_σ^{-1} shows a strongly field-dependent behavior. Effects related to granularity dominate in this region and another scaling behavior, which is due to phase fluctuations in the granular array, may be identified. Particularly, the set of parallel solid straight lines obtained from fitting the χ_σ^{-1} data in Figure 4 corresponds to the asymptotic regime of the coherence transition, where equation (6) is valid.

In Table 1 are shown the values obtained for the critical conductivity exponents from fittings of the data to equation (6). In zero and very low applied field (smaller than 10 Oe, typically), the power law behavior of the conductivity is characterized by the exponent $\lambda \cong 3$ for all of the studied samples, excepting Y123:b where λ is larger. The exponent $\lambda \cong 3$ has been identified in other experiments performed in zero and very low fields [18–22,35]. However, when the magnetic field exceeds a few Oersteds, the value $\lambda \cong 4$ is generally found [9,20,21]. Sample Y123:b, listed in Table 1, is a rare exception. In this case, the high value found for this exponent ($\lambda \cong 5$) suggests that an exponential conductivity term due to the flow of Abrikosov vortices competes with the power law behavior characteristic of the coherence transition.

4 Discussion

Assuming that the conductivity near the zero resistance state of granular superconductors is dominated by a thermally controlled percolation-like transition, the contribution of thermal fluctuations is characterized by a critical exponent given by [37]

$$\lambda = \nu\,(2 + z - d)\,, \tag{7}$$

Table 1. Parameters for the investigated samples: critical temperature determined from the peak of $d\rho/dT$; resistivity at 100 K; normalized critical amplitude for the coherence transition; critical exponents for the coherence transition in zero applied field and in the presence of a magnetic field.

Sample	T_c (K)	ρ(100 K) (mΩ cm)	A_0 (mΩ cm)	λ ($H = 0$)	λ ($H \neq 0$)
Y123:a	92.3	0.96	1.0 ± 0.1	2.4 ± 0.1	3.8 ± 0.3
Y123:b	92.0	0.8	13.5 ± 3	4.3 ± 0.6	4.9 ± 0.4
Y123:Sr	90.0	0.7	74 ± 7	3.0 ± 0.1	3.7 ± 0.2
Y123:Zn	79.4	1.0	1170 ± 120	3.4 ± 0.4	4.1 ± 0.2

where ν is the critical exponent for the correlation length and z is the dynamical exponent.

The value found for λ near the zero field limit in the Y123:a, Y123:Zn and Y123:Sr systems (see Tab. 1) is in good agreement with predictions of a Monte Carlo study by Wengel and Young [40], based on the 3D-XY phase-glass Hamiltonian given by equation (1). These authors found that in both the gauge-glass and chiral-glass versions of the model based on equation (1), the critical phenomenology is described by the exponents $\upsilon \cong 1.3$ and $z \cong 3.1$. These values imply that $\lambda \cong 3$ according to equation (7).

However, in the presence of a field, the experimental exponent corresponding to the asymptotic coherence regime is $\lambda = 4.0 \pm 0.3$ in our granular systems. This value is in agreement with determinations of earlier experiments [9,20,21,26]. The value $\lambda \cong 4.0$ may be understood within the approach of Wengel and Young [40] if the dynamical exponent undergoes a crossover to $z \cong 4$, which is a value expected for a spin glass-like critical dynamics [41]. A large value for z is also reported in many investigations of the I–V characteristics of granular HTSC [42,43]. We also mention that the experimental $\lambda = 4.0 \pm 0.3$ is in good agreement with the prediction of a Monte Carlo study by Olson and Young [44] for the 3D-gauge glass that gives $\lambda = 4.5 \pm 1.1$. In any case, the conductivity exponents found in our study suggest that the universality class for the coherence transition is that of the 3D-XY model where non-trivial disorder is relevant.

An interesting feature observed in the data of Figure 4 is a systematic downwards deviation of the straight line fits when the zero resistance state is approached. Although one should be aware of the significant uncertainty associated to data in this region because of their numerical determination, if we suppose that χ_σ^{-1} is still described by equation (6), the downwards deviation would correspond to a crossover to a fluctuation regime characterized by an exponent smaller than the fitted λ. This behavior is consistent with the description of the coherence transition within the 3D-XY critical thermodynamics. Indeed, very close to the critical point, the temperature dependent coherence length diverges and eventually becomes larger than the correlation length for the disordered structure. In such a situation, disorder ceases to be relevant and the small 3D-XY exponents of the ordered case should be recovered.

The behavior of the χ_σ^{-1} results in the region above the coherent transition, as shown in Figure 4, strongly suggests that the whole measurements may be scaled as to collapse into a single curve. In order to verify the validity of this assumption, we note that the scaling behavior proposed for the fluctuation conductivity close to the vortex-glass transition is given by [45]

$$\Delta\sigma(T,H) \approx H^{-(2+z-d)/2} S_\pm \left(\frac{t}{H^{1/2\upsilon}} \right), \tag{8}$$

where $t = (T - T_{c0})/T_{c0}$, and $S_\pm$ are scaling functions above and below T_{c0}, respectively.

Following Fischer et al. [37], we assume that

$$[T_c - T_{c0}(H)] \approx H^{1/2\upsilon} \tag{9}$$

and derive

$$\Delta\sigma \approx [T_c - T_{c0}(H)]^{-\upsilon(2+z-d)} F_\pm(\tau), \tag{10}$$

where $F_\pm(\tau)$ are scaling functions of the variable

$$\tau = \frac{T - T_{c0}(H)}{T_c - T_{c0}(H)}. \tag{11}$$

This scaling variable was first introduced by Kötzler et al. [46] for describing the dynamical scaling of the complex electrical conductivity of $YBa_2Cu_3O_{7-\delta}$ near the vortex-glass transition.

From equation (10) we obtain that

$$\frac{d}{d\tau} \ln F_+(\tau) = -\chi_\sigma [T_c - T_{c0}(H)] \tag{12}$$

in the paracoherent region (above T_{c0} and below T_c). In Figure 5 is shown a plot of $\chi_\sigma [T_c - T_{c0}(H)]$ versus τ that was obtained by scaling the data for Y123:a, Y123:b, Y123:Sr and Y123:Zn in all of the studied fields. Good scaling is obtained in most of the range [0,1] for the variable τ. Marked deviations occur close to the high-temperature end of the scaling range, where a steep increase of χ_σ^{-1} is observed in temperatures just below the minimum where T_c is located. This particular regime, though below T_c, is still influenced by fluctuations in the normal phase [9].

The fact that all of our measurements scale as shown in Figure 5 gives support to the description of the regime of approach to the zero resistance state in granular HTSC samples as precursory to a phase transition phenomenon. In order to search for further evidence of the validity of this assumption, we study the critical amplitudes, A_c, for the fluctuation conductivity above T_{c0}, that is,

$$A_c = \Delta\sigma / t^{-\lambda}. \tag{13}$$

We derive the critical amplitudes from the experimental data in the asymptotic temperature interval just above T_{c0}, where the exponent λ is determined. We obtain that A_c is an increasing function of the applied magnetic field (see Fig. 6). We also found that the values for A_c are

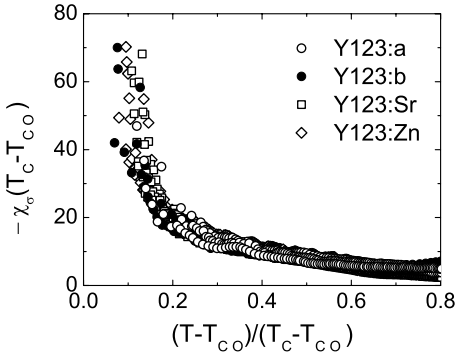

Fig. 5. Scaling of the fluctuation conductivity based on equation (12) in the coherence regime between T_{c0} and T_c for the Y123a, Y123b, Y123:Sr and Y123:Zn samples. The whole set of results obtained in magnetic fields ranging from 0 to 400 Oe are plotted.

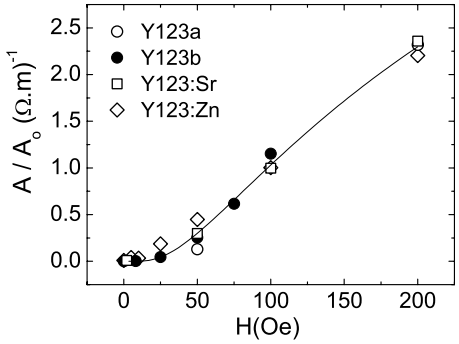

Fig. 6. Normalized critical amplitudes of the fluctuation conductivity in the asymptotic coherence regime as functions of the applied field. The continuous line is calculated with equation (14) using the exponent $\eta = 0.6 \pm 0.2$. The fitting parameters A_0 are quoted in Table 1.

strongly sample dependent. This is not surprising since the coherence transition is a percolation-type process. Then, the resistivity in this regime is expected to be extremely sensitive to particularities of the sample's granularity. In Figure 6 we show the critical amplitudes normalized as A_c/A_0 versus the applied field for the Y123:a, Y123:b, Y123:Zn and Y123:Sr samples. We arbitrarily choose $A_0 = 1$ for the Y123:a sample measured in the field $H = 100$ Oe. The values for A_0 for the other samples are determined so that the data collapse into a single plot. The values found for A_0 are listed in Table 1. In Figure 6 these data are phenomenologically fitted to

$$A_c\,(H) = A_0 e^{-a/H^\eta}, \qquad (14)$$

where a is a constant. Equation (14) mimics the behavior of the nonlinear voltage response near the vortex-glass transition with the longitudinal H playing a role similar to that of the current density [32,42]. From the fit of the amplitude data to equation (14), we obtain $\eta = 0.6 \pm 0.2$. This value is within the expectations of the vortex-glass theory [32,42].

Equation (14) predicts that $A_c(H)$ tends to zero in the $H = 0$ limit. Experimentally, however, we find a small value for this amplitude in zero applied field. This might be originated by the fact that in a resistivity experiment the self-field can not be eliminated and its value may be non-negligible at the constrictions between grains. We also note that a change in the value of the critical conductivity exponent is observed in experiments performed at zero and very low applied fields.

It is interesting to observe in Table 1 that the values fitted for A_0 in the studied systems span three orders of magnitude and are not directly related to the absolute values of the resistivity in the normal phase (the resistivities at 100 K are also listed in Tab. 1). The Y123:Zn system presents the highest value for A_0, although its resistivity at 100 K is about the same as for the other samples. However, in Y123:Zn the critical temperature is the lowest and the granularity effects are the most pronounced, as may be seen in Figures 1 and 3. The Zn-doping induces granularity at the microscopic level. A consequence of this fact is the shortening of the correlation length ξ_C for the order parameter of the coherence transition, as we expect that ξ_C is basically given by the size of the superconducting grain (region where superconductivity is homogeneous). The value for A_0 in the Y123:Sr sample is more than one order of magnitude lower when compared to that in the Zn-doped system. The Sr-doping is not as effective as the Zn-doping to improve the granularity in Y123 probably because the impurities locate out of the Cu-O_2 atomic planes in the former case. However, the value for A_0 in the Y123:Sr is significantly larger than that for the pure Y123:b sample. The amplitude A_0 is still smaller in our 'best quality' Y123:a sample. Thus, the value of A_0 seems related to the strength of granularity in our samples as estimated by the temperature width and field sensibility of the regime of approach to the zero resistance state, the value of T_c, and other properties.

A possible outcome of our experiments and analyses is that ξ_C is inversely proportional to A_0. In other words, the typical size of the superconducting grains is much smaller in Y123:Zn than in the other investigated samples, and tends to increase as the system becomes pure and well ordered. Moreover, the fact that A_0 is an increasing function of H, as shown in Figure 6, gives additional support to this interpretation. Indeed, the longitudinal magnetic field is expected to decouple the superconducting clusters, thus shortening ξ_C.

5 Conclusions

We have experimentally studied the regime of approach to the zero resistance state in granular samples of $YBa_2Cu_3O_{7-\delta}$, $YBa_{1.75}Sr_{0.25}Cu_3O_{7-\delta}$ and $YBa_2Cu_{2.95}Zn_{0.05}O_{7-\delta}$. The temperature derivative of the resistivity near T_c reveals that the transition of the studied systems is a two-stage process. We found that besides producing a dramatic depression of T_c, the Zn-doping causes a significant enlargement of the resistive transition, which is probably due to an enhancement of granularity effects at the microscopic length scale. We also notice a relatively

small but sizeable reduction of T_c and enlargement of the transition in the Y123:Sr sample.

Our fluctuation conductivity results under longitudinal magnetic fields are interpreted by assuming that a coherence transition related to phase fluctuations of individual grains of the disordered granular array occurs at a characteristic critical temperature, $T_{c0}(H)$. This temperature is located well below the pairing critical temperature, T_c. The state with zero-resistance stabilizes below T_{c0}, where a phase coherent and long-range ordered state is established in the whole granular array.

Extended power law regimes corresponding to critical fluctuations of the conductivity under longitudinal magnetic fields are identified in the regime of approach to the zero-resistance state. In zero and very low applied fields, these fluctuations are described by the exponent $\lambda \cong 3$. With application of magnetic fields above a very low threshold the exponent changes to $\lambda \cong 4$. The obtained exponents indicate that the static and dynamic universality classes for the coherence transition is that of the 3D-XY model described by the phase-glass Hamiltonian of equation (1), where the disorder is nontrivial and critically relevant. The data could be described by a vortex-glass type of scaling. This fact suggests that the coherence transition in our granular superconductors fits into the more general framework of the vortex-glass theory. The critical amplitude for the fluctuation conductivity in the regime above the coherence transition was analyzed for the first time. Its field dependence qualitatively reproduces the predicted behavior for the non-linear voltage response near a vortex-glass transition [37]. The variation of the magnitude of the critical amplitude A_0 along the series of investigated samples lead us to suggest that this amplitude is inversely proportional to the correlation length characteristic of the coherence transition.

References

1. J. Mannhart, P. Chaudari, D. Dimos, C.C. Tsuei, T.R. McGuire, Phys. Rev. Lett. **61**, 2476 (1988)
2. R. Gross, P. Chaudari, D. Dimos, A. Gupta, G. Koren, Phys. Rev. Lett. **64**, 228 (1990)
3. H. Hingenkamp, J. Mannhart, Rev. Mod. Phys. **74**, 485 (2002)
4. K.M. Lang, V. Madhavan, J.E. Hoffman, E.W. Hudson, H. Eisaki, S. Uchida, J.C. Davis, Nature **415**, 412 (2002)
5. E. Liarokapis, D. Palles, D. Lampakis, G. Böttger, K. Conder, E. Kaldis, Phys. Rev. B **71**, 014303 (2005)
6. M. Daeumling, J.M. Seuntjens, D.C. Larbalestier, Nature **346**, 332 (1990)
7. A Gerber, T. Grenet, M. Cyrot, J. Beille, Phys. Rev. Lett. **65**, 3201 (1990)
8. P. Pureur, J. Schaf, M.A. Gusmão, J.V. Kunzler, Physica C **176**, 357 (1991)
9. J. Roa-Rojas, R. Menegotto Costa., P. Pureur, P. Prieto, Phys. Rev. B **61**, 12457 (2000)
10. A. Raboutou, P. Peyral, C. Lebeau, J. Rosenblatt, J.P. Burin, Y. Fouad, Physica A **207**, 271 (1994)
11. J. Rosenblatt, P. Peyral, A. Raboutou, C. Lebeau, Physica B **152**, 95 (1988)
12. M.P.A. Fischer, T.A. Tokuyasu, A.P. Young, Phys. Rev. Lett. **66**, 2931 (1991)
13. W.Y. Shih, C. Ebner, D. Stroud, Phys. Rev. B **30**, 134 (1984)
14. H. Kawamura, M.S. Li, J. Phys. Soc (Jpn) **66**, 2110 (1997)
15. M. Siegrist, T.M. Rice, Rev. Mod. Phys. **67**, 503 (1995)
16. L.N. Bulaevskii, V.V. Kuzii, A.A. Sobyanin, Solid State Commun. **25**, 1053 (1978)
17. B.I. Spivak, S.A. Kivelson, Phys. Rev. B **43**, 3740 (1991)
18. P. Peyral, C. Lebeau, J. Rosenblatt, A. Raboutou, C. Perrin, O. Peña, M. Sergent, J. Less-Common Met. **151**, 151 (1989)
19. J. Roa-Rojas, P. Pureur, L. Mendonça-Ferreira, M.T.D. Orlando, E. Baggio-Saitovitch, Supercond. Sci. Technol. **14**, 898 (2001)
20. F.W. Fabris, J. Roa-Rojas, P. Pureur, Physica C **354**, 304 (2001)
21. F. Wolff Fabris, P. Pureur, Physica C **408–410** 688 (2004)
22. P.K. Nayak, S. Ravy, Solid State Commun. **140**, 464 (2006)
23. M. Kaur, R. Srinivasan, G.K. Mehta, D. Kanjilal, R. Pinto, S.B. Ogale, S. Mohan, V. Ganesan, Physica C **443**, 61 (2006)
24. A.R. Jurelo, I. Abrego Castillo, J. Roa-Rojas, L.M. Ferreira, L. Ghivelder, P. Pureur, P. Rodrigues Jr, Physica C **311**, 133 (1999)
25. C.J. Lobb, Phys. Rev. B **36**, 3930 (1987)
26. P. Pureur, R. Menegotto Costa, P. Rodrigues, Jr, J. Schaf, J.V. Kunzler, Phys. Rev. B **47**, 11420 (1993)
27. R. Menegotto Costa, P. Pureur, L. Ghivelder, J.A. Campá, I. Rasines, Phys. Rev. B **56**, 10836 (1997)
28. R. Menegotto Costa, P. Pureur, M. Gusmão, S. Senoussi, K. Behnia, Phys. Rev. B **64**, 214513 (2001)
29. B. Jayaram, S.K. Agarwal, C.V.N. Rao, A.V. Narlikar, Phys. Rev. B **38**, 2903 (1988)
30. S. Zagoulev, P. Monod, J. Jégoudez, Phys. Rev. B **52**, 10474 (1995)
31. H. Kimura, Physica C **392–396**, 34 (2003)
32. Y. Zhao, H. Zhang, T. Zhang, S.F. Sun, Z.Y. Chen, Q.R. Zhang, Physica C **152**, 513 (1988)
33. Y. Takeda, R. Kando, O. Yamamoto, M. To, Z. Hiroi, Y. Bando, M. Shimita, H. Akinaga, K. Takita, Physica C **157**, 358 (1989)
34. V.N. Vieira, P. Pureur, J. Schaf, Physica C **353**, 241 (2001)
35. A.R. Jurelo, J.V. Kunzler, J. Schaf, P. Pureur, J. Rosenblatt, Phys. Rev. B **56** 14815 (1997)
36. B. Nachumi, A. Keren, K. Kojima, M. Larkin, G.M. Luke, J. Merrin, O. Tchernyshöv, Y.J. Uemura, N. Ichikawa, M. Goto, S. Uchida, Phys. Rev. Lett. **77** 5421 (1996)
37. D.S. Fischer, M.P.A. Fischer, D.A. Huse, Phys. Rev. B **43**, 130 (1991)
38. M. Ausloos, Ch. Laurent, Phys. Rev. B **37**, 611 (1988)
39. J.S. Kouvel, M.E. Fisher, Phys. Rev. **136**, A1616 (1964)
40. C. Wengel, A.P. Young, Phys. Rev. B **56**, 5918 (1997)
41. A. Zippelius, Phys. Rev. B **29**, 2717 (1984)
42. S. Li, M. Fistul, J. Deak, P. Metcalf, M. McElfresh, Phys. Rev. B **52**, (1995) R747
43. R.J. Joshi, R.B. Hallock, J.A. Taylor, Phys. Rev. B **55**, 9107 (1997)
44. T. Olson, A.P.Young, Phys. Rev. B **61**, 12467 (2000)
45. M.B. Salamon, Jing Shi, Neil Overend, M.A. Howson, Phys. Rev. B **47**, 5520 (1993)
46. J. Kötzler, M. Kaufmann, G. Nakielski, R. Behr, W. Assmus, Phys. Rev. Lett. **72**, 2081 (1994)
47. M.P.A. Fischer, Phys. Rev. Lett. **62**, 1415 (1989)